J Mater Sci: Mater Med (2015) 26:235
DOI 10.1007/s10856-015-5567-3

BIOMATERIALS SYNTHESIS AND CHARACTERIZATION

Original Research

Phytosynthesis of gold nanoparticles using *Mappia foetida* leaves extract and their conjugation with folic acid for delivery of doxorubicin to cancer cells

S. Yallappa[1] · J. Manjanna[2] · B. L. Dhananjaya[3] · U. Vishwanatha[4] · B. Ravishankar[4] · H. Gururaj[5]

Received: 20 April 2015 / Accepted: 16 September 2015 / Published online: 22 September 2015

Abstract *Mappia foetida* leaves extract is used as bioreductant for the synthesis of gold nanoparticles and their application in the efficient delivery of doxorubicin to human cancer cells is reported here. The formation of gold nanoparticles is evident from their characteristic optical absorption at ~560 nm. X-ray diffraction pattern of gold nanoparticles confirmed their *fcc* structure. Fourier transform infrared spectroscopy shows the bioactive molecules from plant extract capped on the surface of gold nanoparticles and conjugation of doxorubicin along with activated folic acid as navigational molecules for targeted drug delivery. Such a conjugation of gold nanoparticles is characterized by their weight loss, ~35–40 %, due to thermal degradation of plant biomass and conjugated drug along with receptor, as observed in thermogravimetric analysis. The spherical shaped gold nanoparticles (Φ 10–20 nm) are observed by field emission scanning electron microscopy and transmission electron microscopy images and the expected elemental composition by energy dispersive X-ray spectroscopy. Gold nanoparticles conjugated with activated folic acid and doxorubicin complex is found to be toxic for human cancer cells viz., MDA-MB-231, HeLa, SiHa and Hep-G2. Furthermore, the amount of drug released was maximum at pH 5.3 (an ambient condition for intravenous cancer drugs) followed by pH 7.2 and pH 6.8.

1 Introduction

Metal nanoparticles (MNPs) in general find widespread applications in engineering, medicine, environment and agricultural sectors owing to their unique physical and chemical properties [1–3]. The biocompatible gold nanoparticles (AuNPs) have been studied as biosensors, diagnostic agents, cell targeting vectors, heating mediators for cancer thermotherapy and drug delivery vehicles [4–6]. These biomedical applications of AuNPs stems from their less cytotoxicity, high stability, ability to bind biomolecules and also their visible light extension behavior [7, 8]. Furthermore, the surface modification of AuNPs is essential for conjugation with biomolecules such as receptors, drugs etc., for their use in biomedicine because such modifications confers a specific function to the nano-bio conjugate [9]. Thus, it is possible to target tumor cells and enter the cell via receptor mediated endocytosis, so called active targeting [10, 11].

The AuNPs of different sizes and shapes are routinely synthesized by different chemical and physical methods [12, 13]. However, these synthetic approaches have some limitations and negatively impact on the environment and human health [14, 15]. Hence, there has been a constant urge across the world to develop an ideal green protocol. In this context, MNPs synthesis using plant extracts by the so

✉ J. Manjanna
jmanjanna@rediffmail.com

[1] Department of Industrial Chemistry, Kuvempu University, Shankaraghatta 577 451, India

[2] Department of Chemistry, Rani Channamma University, Belagavi 591 156, India

[3] Toxicology and Drug Discovery Centre for Emerging Technologies, Jain University, Ramanagara 562 112, India

[4] SDM Centre for Research in Ayurveda and Allied Sciences, Udupi 574 118, India

[5] Department of Electronics, Kuvempu University, Shankaraghatta 577 451, India

called 'green synthesis' has emerged as one of the options for implementing the green chemistry principles and has successfully made an important contribution towards green nanotechnology arena. The synthesis and mechanisms of MNPs using plant extracts are well understood and the success rate of synthesis is very productive and has exhibited assorted applications [16]. Many reports are available on synthesis of highly monodispersed AuNPs using different plant extracts [17–19]. Such a green protocol has several advantages, for instance, thermally and chemically stable, profitable, biocompatible and environmentally friendly. The biosynthesized NPs are found to be adsorbed or functionalized by biological peptides of plant extract, which can also be used as natural bio-linkers for anchoring drugs.

The functionalized NPs can be effectively used for the treatment of various diseases by means of targeted drug delivery i.e., the necessary amount of drug to the targeted site for a necessary period of time, both efficiently and precisely. To design advanced dosage forms, suitable carrier materials are used to overcome the undesirable properties of the drug molecules. The biomedical applications of AuNPs are evident in drug delivery and gene delivery for synapses and controlled release of chemotherapeutic drugs to the diseased sites. This property is facilitated by attaching the drugs to the NPs and allows the use of lower doses of drugs, which are less toxic with improved therapeutic efficacy [20]. Furthermore, AuNPs displays remarkable conjugation capabilities due to their large surface area which allows them to bind various chemical compounds including drugs, proteins and other molecules by covalent bonds [21].

Among the cancer chemotherapeutics, doxorubicin (DOX) is a widely used anticancer drug and it kills the cancerous cells by inhibiting the synthesis of nucleic acids within cells. The folic acid is used as a navigational molecule [22] and has been reported for the construction of molecular Trojan horses, through which drugs or ligands can be attached. Folic acid conjugated NPs have been found to target cancer cells, which over express folate receptors on their surfaces [23]. This property enables the conjugation of NPs to the folate receptors and gets internalized via an endocytosis mechanism. As such, nanoparticulate drugs will be able to reach their target more efficiently at a lower concentration resulting in faster drug onset and lesser side effect that are beneficial to the patient. However, there are many studies [24–27] on utilizing folic acid as receptors in nano-carriers for the active targeting of cancer cells. Nevertheless, there are only a few reports [19] on biosynthesized AuNPs conjugated anticancer drugs along with folic acid as receptor for targeted drug delivery and their response in biosystem.

Mappia foetida (*M. foetida*) commonly known as Narakya is one such ethno medicinally important evergreen tree used for treatment of various diseases viz, skin diseases, mental illness, tuberculosis, diabetes, jaundice, hypertension and cancer [28]. Furthermore, the chemical compound such as camptothecin isolated from *M. foetida* was used for the treatment of lung, ovarian and cervical cancer [29]. To our knowledge, synthesis of AuNPs using *M. foetida* leaves extract under microwave irradiation has not been reported hitherto. Thus, we report on phytosynthesis of AuNPs as nano-vehicles for delivering DOX to solid tumors (cancer cell lines) using folic acid as receptor. In addition, the drug loading and drug release kinetics are presented here.

2 Materials and methods

2.1 Materials

Fresh leaves of *M. foetida* leaves were collected from the Muroor hills of Kumta in Karnataka, India. Chloroauric acid ($HAuCl_4$) and DOX drug were purchased from Sigma Aldrich Laboratory (Bangalore, India) and were used as received. Folic acid, n-hydroxy succinamide (NHS), dicarboxy aminocarbodiimide (DCC), 3-(4,5-dimethyl-2-thiazolyl)-2,5-diphenyl-2H-tetrazolium bromide (MTT), fetal calf serum (FCS), modified Eagles medium (MEM), glutamine, EDTA, trypsin, dimethyl sulfoxide (DMSO) and methanol of analytical grade were purchased from Himedia Laboratory, Bangalore, India. The different cancer cell lines such as MDA-MB-231 (breast), HeLa (cervix), SiHa (cervix) and Hep-G2 (liver) and normal epithelial Vero cell lines were procured from National Centre for Cell Science (NCCS), India.

2.2 Preparation of aqueous *M. foetida* leaves extract

A 10 g of *M. foetida* leaves were thoroughly washed with distilled water and cut into small pieces. It was added to 200 ml of distilled water in a 500 ml beaker and subjected to microwave irradiation for about 180 s to extract the phytochemicals present in the leaves. It was filtered through 0.22 μm membrane filter in hot condition to get a clear extract. The filtrate was cooled to room temperature and used as bio-reductant for the synthesis of AuNPs.

2.3 Synthesis of AuNPs

For synthesis of AuNPs, 10 ml of freshly prepared *M. foetida* leaves extract was added to 50 ml of 10^{-3} M aqueous solution of $HAuCl_4$ in a 250 ml beaker. The mixture was subjected for microwave irradiation at full

power (700 W, 2.45 GHz) to different intervals of time. The formation of AuNPs was indicated by color change of the reaction mixture, light yellow to purple after 30 s and then to wine red after 240 s of irradiation.

The formation of AuNPs was monitored by recording UV–Vis absorption spectra (Shimadzu, 1650-PC) for surface plasmon resonance (SPR) peak. UV–Vis analysis was carried for a period of 240 s. In order to understand the reducing ability of the plant extract, the reduction potential (E) and pH of the reaction mixture ($HAuCl_4$ and leaves extract) was measured using digital potentiometer and pH meter, respectively. The synthesized AuNPs was collected by centrifuging the colloidal solution at 5000 rpm for 30 min. The solid residue thus obtained here was repeatedly washed with distilled water to remove the unbounded bioactive molecules to the surface of NPs, which are not responsible for biofunctionalization. The resultant residue was dried in vacuum oven at 80 °C for about 12 h to obtain the same in powder form. Further, it was well characterized by using various physico-chemical techniques as given in below section.

2.4 Activation of folic acid and its conjugation with AuNPs

The activation of folic acid was done by the previous reported method as follows [19]. Briefly, 0.25 g of folic acid was dissolved in 20 ml of DMSO using sonication for 30 min to get a clear dilution. To this solution, 0.225 g of NHS and 0.125 g of DCC was added for the activation of carboxyl group in folic acid (folic acid/NHS/DCC molar ratio 2:2:1). The reaction mixture was allowed to stir for 2 h in nitrogen atmosphere. The product obtained was filtered through Whatman filter paper no. 42 and dried at room temperature. The dried powder was characterized by nuclear magnetic resonance (NMR) and Fourier transform infrared (FT-IR) spectroscopy for confirmation of activated folic acid (folic acid is modified with NHS) and then used for the conjugation of AuNPs.

For conjugation with AuNPs, 0.1 g each of activated folic acid (FA–NHS) and biosynthesized AuNPs was taken in beaker containing 20 ml of distilled water. The mixture was kept for stirring under nitrogen atmosphere for about 24 h. After completing the reaction, AuNPs conjugated folic acid (AuNPs–FA–NHS) was collected by centrifuging at 5000 rpm for 30 min. The free folic acid was removed by using a 3000 kDa dialysis tube in phosphate buffer saline at pH 6.9. The post-dialyzed samples were then centrifuged at 5000 rpm for 30 min. The AuNPs conjugated folic acid thus obtained here was repeatedly washed with distilled water and dried in vacuum oven at 30–40 °C for about 24 h to obtain the same in powder form.

2.5 Conjugation of DOX to AuNPs–FA–NHS

A 2.5 mg of DOX was dissolved in 5.0 ml of phosphate buffer solution at pH 7. Then, 25 mg of AuNPs–FA–NHS was mixed with 5.0 ml drug solution (drug concentration = 1.0 mg/ml) and the mixture was kept on stirring under nitrogen atmosphere for about 2 h. The resultant solution was placed in a rotary shaker at 200 rpm for 24 h and subsequently freeze-dried for 48 h. The synthesis steps for the activation of folic acid and conjugation process with AuNPs and anticancer drug is as shown in Scheme 1.

2.6 Drug loading efficiency

In order to know the drug loading efficiency, 5.0 ml of DOX attached AuNPs (i.e., AuNPs–FA–NHS–DOX) from previous experiment was sealed in porous dialysis tube and was dialyzed against distilled water for 24 h. The released drug concentration was monitored by recording UV–Vis spectrophotometer. The drug loading efficiency was calculated as follows:

$$\text{Drug loading efficiency} = \frac{\text{Total amount of drug loaded} - \text{amount of drug released}}{\text{Total amount of drug loaded}} \times 100.$$

2.7 Drug releasing studies

A 5.0 ml of dialyzed AuNPs–FA–NHS–DOX complex was sealed in three different porous dialysis tubes and placed separately in a beaker containing 50 ml of phosphate buffer solution at different pH (5.3, 6.8 and 7.2) with continuous stirring at 100 rpm. The entire system was kept in an incubator at 37 °C. To measure the drug release content, 1.0 ml samples were periodically removed and replaced with an equivalent volume of phosphate buffer solution. The amount of drug released was monitored by recording UV–Vis spectrophotometer at ~485 nm. The experiments were done in triplicate and mean values were calculated.

2.8 Characterization techniques

The powder X-ray diffraction (XRD, Siemens X-ray diffractometer, Japan) pattern of biosynthesized AuNPs was recorded using 'X'PERT-PRO XRPD (Cu Kα, $\lambda = 0.15406$ nm) with a scanning rate of 2°/min and 2θ ranging from 10° to 70°. The structural morphology of AuNPs was observed by using field emission scanning electron microscopy (FESEM, FEI Nova nano 600, The Netherlands), operated at 15 keV and transmission electron microscopy (TEM CM-200, Philips) operated at 190 keV. The energy-dispersive X-ray (EDX) analysis was used for

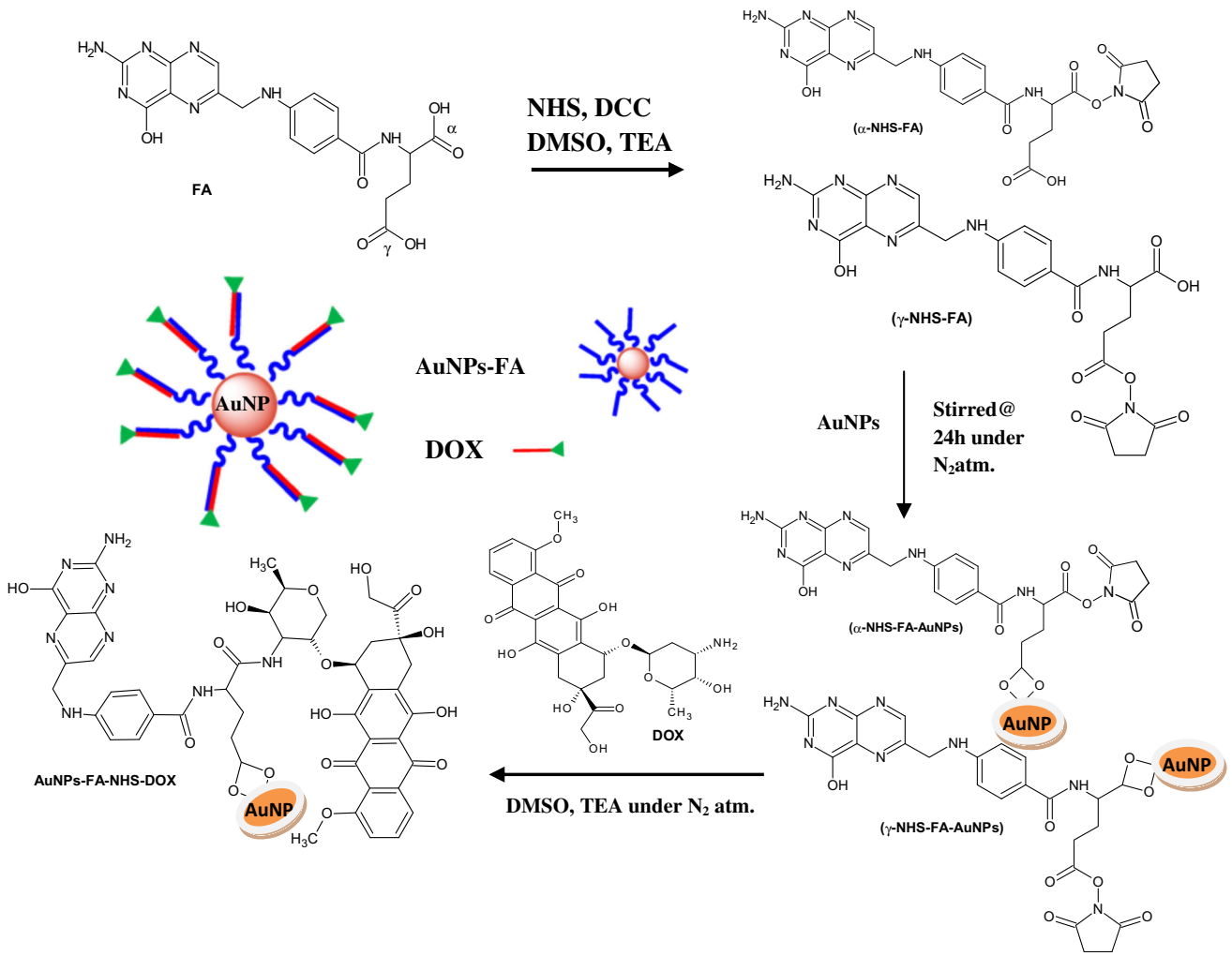

Scheme 1 The synthesis steps for the activation of FA and conjugation with AuNPs and DOX

elemental composition. A ^{1}H NMR spectrum (Bruker, DRX 300 MHz) was recorded to confirm the activation of folic acid for conjugation with AuNPs and drug. Fourier transform infrared (FT-IR, Bruker-TENSOR 27) spectra were recorded at a spectral resolution of 4 cm^{-1} in KBr pellet to know the functionalization of bioactive molecules from plant extract on AuNPs with activated folate and anticancer drug. The thermogravimetric (TG, Linseis STA PT1600, Germany) curve was traced under nitrogen atmosphere with a heating rate of 10 °C/min to determine the amount of plant biomass adsorbed and drug loaded onto AuNPs through thermal degradation.

2.9 In-vitro cytotoxic activity

2.9.1 Cell culture

The different cell lines namely MDA-MB-231, HeLa, SiHa and Hep-G2 (human cancer cells) and epithelial Vero cell lines (normal cells) were maintained in MEM supplemented with 10 % FCS, 2 % essential amino acids, 1 % each of glutamine, non essential amino acids, vitamins and 100 U/ml penicillin–streptomycin. Cells were sub cultured at 80–90 % confluence and incubated at 37 °C in a humidified incubator supplied with 5 % CO_2. The stock cells were maintained in 75 cm^2 tissue culture flask.

2.9.2 Cell viability assay

The cytotoxicity effect of AuNPs before and after their conjugation was evaluated by MTT (colorimetric) assay as follows [30]. This is based on the mitochondrial enzyme mediated conversion of pale yellow MTT to violet formazan crystals, which is measured in spectrophotometer. The cultured cells (1×10^{-6} cells/ml) were placed in 96 flat-bottom well plates. Then these cells were exposed to different concentration of prepared nanomaterials (1–100 µg/ml) and incubated at 37 °C for about 24 h in 5 %

CO_2 atmosphere. After 24 h incubation, MTT (10 µl) was added and incubation was continued for 4 h. Thereafter, the formazan crystals were dissolved in 200 µl of DMSO and the absorbance was monitored using microplate reader at a wavelength of 578 nm with the reference filter as 630 nm. The cytotoxicity effect was calculated as:

$$\text{Cytotoxicity}(\%) = 1 - \left(\frac{\text{Mean absorbance of toxicant}}{\text{Mean absorbance of } -\text{ve control}}\right) \times 100$$

$$\text{Cell viability } (\%) = 100 - \text{Cytotoxicity } (\%).$$

2.10 Statistical analysis

A statistical analyses values for all the experiments were expressed as ±standard deviation. The data were performed using Student's *t* test, where statistical significance was calculated for treated samples and untreated (as control) cells.

3 Results and discussion

3.1 Formation of AuNPs

The color of the reaction mixture (50 ml of 1 mM $HAuCl_4$ + 10 ml plant extract) turned from light yellow to wine red within 90 s of microwave irradiation. The AuNPs shows wine red color in aqueous medium is due to SPR of MNPs [31]. The intensity of the reaction mixture increased with microwave irradiation time until about 180 s and the saturation point was reached in about 240 s. As shown in Fig. 1, the λ_{SPR} varied from 560 to 550 nm with increasing irradiation time [32]. Such a slight blue shift is due to increase in particle size as the yield of AuNPs increased with reaction time. The photos in the inset of Fig. 1 show the color or intensity of reaction mixture on microwave irradiation to 10, 30 and 240 s. The maximum reduction ($Au^{3+} \rightarrow Au^0$) occurred within 180 s and beyond which there was a marginal increase in SPR intensity. During this process, bioactive molecules present in the plant extract spatially controlled the nucleation and growth of the particles size leading to AuNPs. The microwave irradiation increases the rate of the reaction and plays a very important role in the formation of uniform sized particles as reported in the subsequent sections on microstructural analysis here. It is not common to obtain uniform particles by conventional chemical methods. Thus, the present method of green synthetic approach is advantageous as micro-structurally controlled MNPs are obtained. These uniform particles are of great interest for their applications with or without bio-conjugation. In the absence of microwave irradiation, Bhat et al. [17] and Dauthal et al. [33] have reported 4–24 h for the formation AuNPs using *Mushroom* and *Prunus domestica* extracts, respectively.

The pH and redox potential (*E*) of the reaction mixture was measured here to understand the formation mechanism of AuNPs by using plant extracts as reducing agent. This procedure is useful for choosing the suitable plant extracts instead of arbitrary selection. As shown in Fig. 2, the initial $E = 0.019$ V increased to 0.045 V after 240 s of microwave irradiation. Such an increase in *E* to a more positive value, although marginally, indicates the depletion of bio-reductant in the *M. foetida* leaves extract for $Au^{3+} \rightarrow Au^0$. In addition, the initial pH 5.6 of the reaction mixture decreased to pH 3.9 due to the release of H^+ ions during the oxidation of bio-reductant. A similar observation is made in our previous reports for Ag [32] and CuNPs [34]

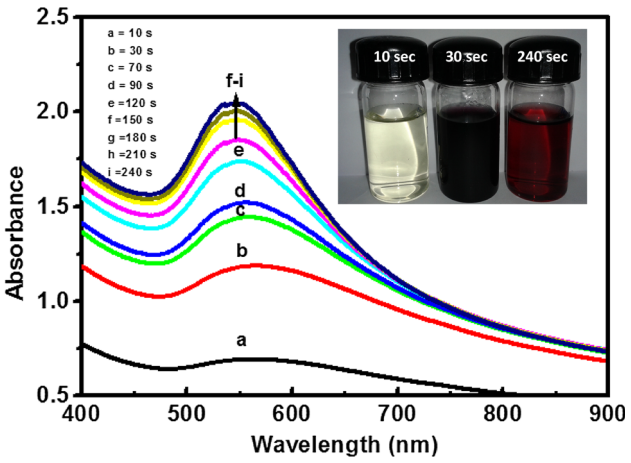

Fig. 1 UV–Vis spectra of the reaction mixture showing the SPR peak 560 nm for AuNPs, *inset* shows the reaction mixture irradiated to 10, 30 and 240 s

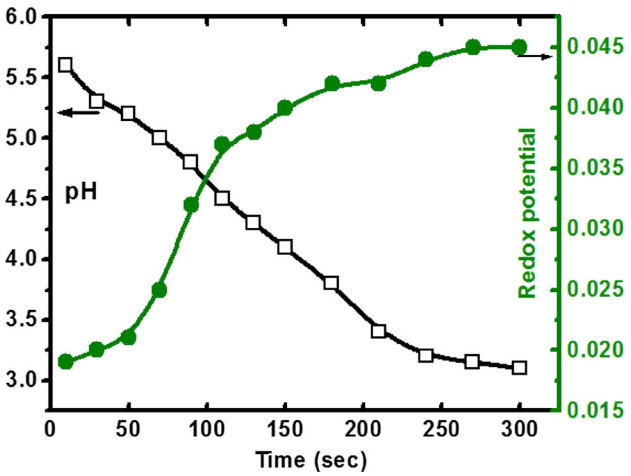

Fig. 2 Variation of redox potential and pH of the reaction mixture as a function of irradiation time

obtained by using *Jasminum sambac* leaves extract and *Terminalia arjuna* bark extract, respectively.

Figure 3 shows the powder XRD pattern of AuNPs synthesized here. The prominent diffraction peaks at $2\theta = 38.55°$, 44.88° and 65.07° can be indexed to (111), (200) and (220) of face centered cubic (*fcc*) structured Au metal (JCPDS file no. 04-0784) [35]. The crystallite size *d* of AuNPs are calculated to be ~10–20 nm using Scherer formula: $d = K\lambda/\beta \cos\theta$, where K—shape factor between 0.9 and 1.1, λ—incident X-ray wavelength (Cu Kα = 1.542 Å), β—full width half-maximum in radians of the prominent line and θ—position of that line in the pattern.

3.2 Conjugation of AuNPs with activated folic acid and DOX

AuNPs were conjugated with FA and DOX yielding AuNPs–FA–NHS–DOX as follows. FA was activated [19] with NHS and the resulting FA–NHS was isolated and characterized. In the next step, the FA–NHS was reacted with AuNPs and DOX to yield AuNPs–FA–DOX complex as represented in Scheme 1. Figure 4 shows the ^{1}H NMR spectra of FA–NHS in comparison with FA derivatives containing the NHS ester group. It is clear that all the peaks have appeared as expected from their structural features. For instance, the methylene protons (**h**) and glutamate portion of FA (**g**) are major groups. The NHS ester formation at the γ and α carboxylates of FA is evident from a new peak **j** (the methylene protons of the NHS) at δ 2.6. The ^{1}H NMR (300 MHz, DMSO-d_6 δ:ppm) peaks can be summarized as: δ 8.65 (1.0 H, s, CH), 8.13 (0.4 H, dd, NH), 7.64 (2.1 H, m, CH), 7.00 (1.4 H, m, NH), 6.65 (2.0 H, m, CH), 4.48 (2.2 H, d, CH2), 4.35 (0.4 H, m, CH), 2.80 (2.6 H, s CH_2), 2.31 (0.6 H, m, CH_2). The ^{1}H NMR spectra

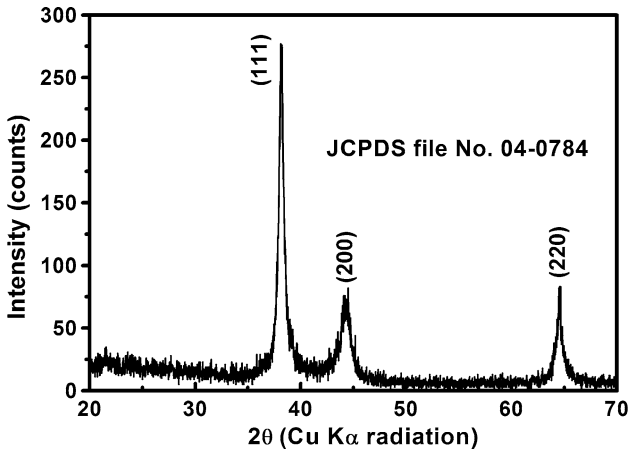

Fig. 3 Powder XRD pattern of AuNPs

results here are in good agreement with earlier report on activation of folic acid with NHS [36].

The UV–Vis spectra of AuNPs, FA–NHS, DOX and AuNPs–FA–DOX are given in Fig. 5. The SPR peaks for AuNPs (~560 nm), FA–NHS (~282 and 364 nm) and DOX (~295 and 485 nm) can be seen clearly. For AuNPs–FA–DOX suspension, the SPRs shifted to 600; 290 and 380; 300 and 510 nm, respectively. This is a clear indication for AuNPs conjugation with FA–NHS and DOX. Such a conjugation is corroborated from different techniques, FESEM/TEM, EDAX, TG analysis and FT-IR as discussed below.

Figure 6 shows the FESEM/TEM (inset) images and EDAX spectra of AuNPs before and after conjugation of DOX. It is clear that the particles are of spherical in shape and there is a narrow size distribution with a diameter (ϕ) in the range of 20–50 nm in each of the case, which is ideal for drug delivery application. The effective drug delivery into the pulmonary system can be achieved through spherical shaped NPs with a diameter <50 nm [37]. No significant differences in morphology of AuNPs were observed before and after conjugation. However, we can see that a thin layer of scum is surrounded on AuNPs and such a scum is more in drug conjugated AuNPs. This is ascribed to bio-capping of organic moieties or phytoconstituents from the plant extract and anchored drug molecules, respectively. The elemental composition from the corresponding EDAX spectra shows about 85 % of AuNPs and the remaining as C and Cl due to bio-capping [17, 18, 32]. Such a bio-capping (medicinally important bioactive molecules) on AuNPs helps to protect them from agglomeration, and also act as natural bio-linkers for anchoring drug molecules.

Figure 7 shows the comparative wt. loss in TG curves for as synthesized AuNPs, AuNPs–FA–NHS and AuNPs–FA–NHS–DOX complex heated from RT to 800 °C under nitrogen atmosphere. The initial wt. loss of ~5 % in each case at <100 °C is ascribed due to the adsorbed water molecules. From 100 to 300 °C, the wt. loss for AuNPs (~15 %), AuNPs–FA–NHS (~20 %) and AuNPs–FA–NHS–DOX (~25 %) could be ascribed to thermal degradation of surface adsorbed plant based bioactive molecules followed by organic molecules such as folic acid and drug. Thereafter, we see a gradual wt. loss up to 600 °C. The overall wt. loss was ~25 % up to 800 °C for AuNPs and ~30–35 % for AuNPs–FA–NHS and AuNPs–FA–DOX. Therefore, the TG analysis here confirms that the drug loaded to AuNPs via conjugation is an efficient. The fact that there was no weight gain is an indication that the NPs remained intact without any oxidation because of the inert atmosphere, nitrogen.

As shown in Fig. 8, the FT-IR spectra of AuNPs shows the broad peaks at 3453 and 2915 cm^{-1} for O–H stretching

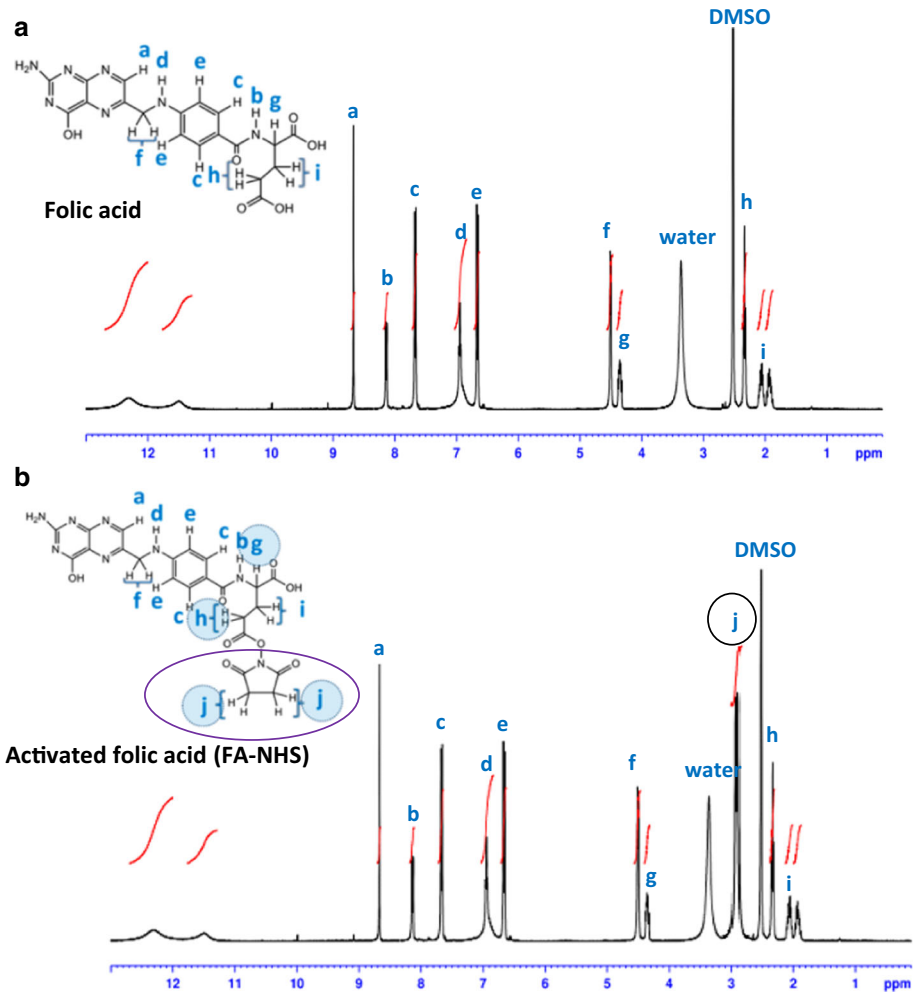

Fig. 4 ^{1}H NMR spectra of **a** pure folic acid and **b** activated folic acid, FA–NHS

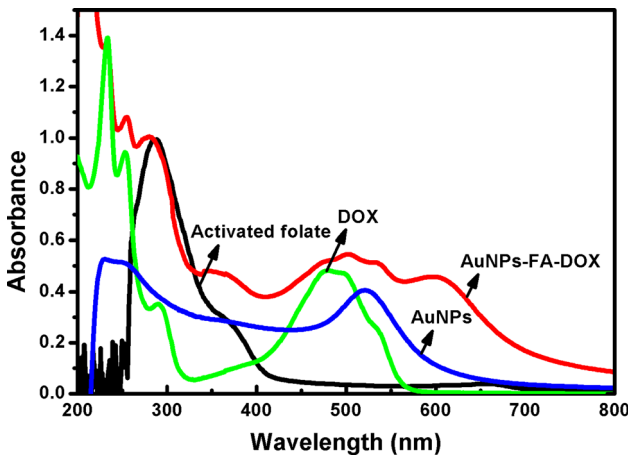

Fig. 5 UV–Vis spectra of AuNPs, activated folate (FA–NHS), DOX and AuNPs–FA–NHS–DOX complex

and the bands at 1645 cm^{-1} (amide group from carbonyl stretch in proteins), 1712 cm^{-1} (C=O stretching) and 1030 cm^{-1} (C–O bending). All these indicate the presence of major bioactive molecules such as polyphenols, favonones and terpenoids from *M. foetida* leaf extract adsorbed on AuNPs [38–40]. The FT-IR spectra of pure folic acid is characterized by bands occurring at 3543, 3415, 3326, 2955, 2840, 1700, 1640, 1488 and 1410 cm^{-1}. The bands between 3600 and 3000 cm^{-1} are due to –OH stretching and –NH stretching vibration bands. The bands appear at 1700 cm^{-1} attributed to C=O bond stretching vibration of carboxyl group, while the band at 1640 cm^{-1} belongs to the C=O bond stretching vibration of –CONH$_2$ group. The band at 1410 cm^{-1} corresponds to –OH deformation of phenyl skeleton and the band at 1484 cm^{-1} is attributed to characteristic absorption of the phenyl ring. Similar peak pattern is seen for FA–NHS also. In case of AuNPs–FA–NHS, the appearance of a broad peak at 1600 cm^{-1} corresponds to asymmetric bending vibrations of –CO and –NH stretching of primary amines. This indicates that folic acid is conjugated with AuNPs by an amide linkage [19]. Furthermore, AuNPs–FA–NHS–DOX interaction is speculated to occur via non-covalent bonding involving carboxylic and amide functional groups. This is evident from 1665 cm^{-1} (=CO stretching of amide) and

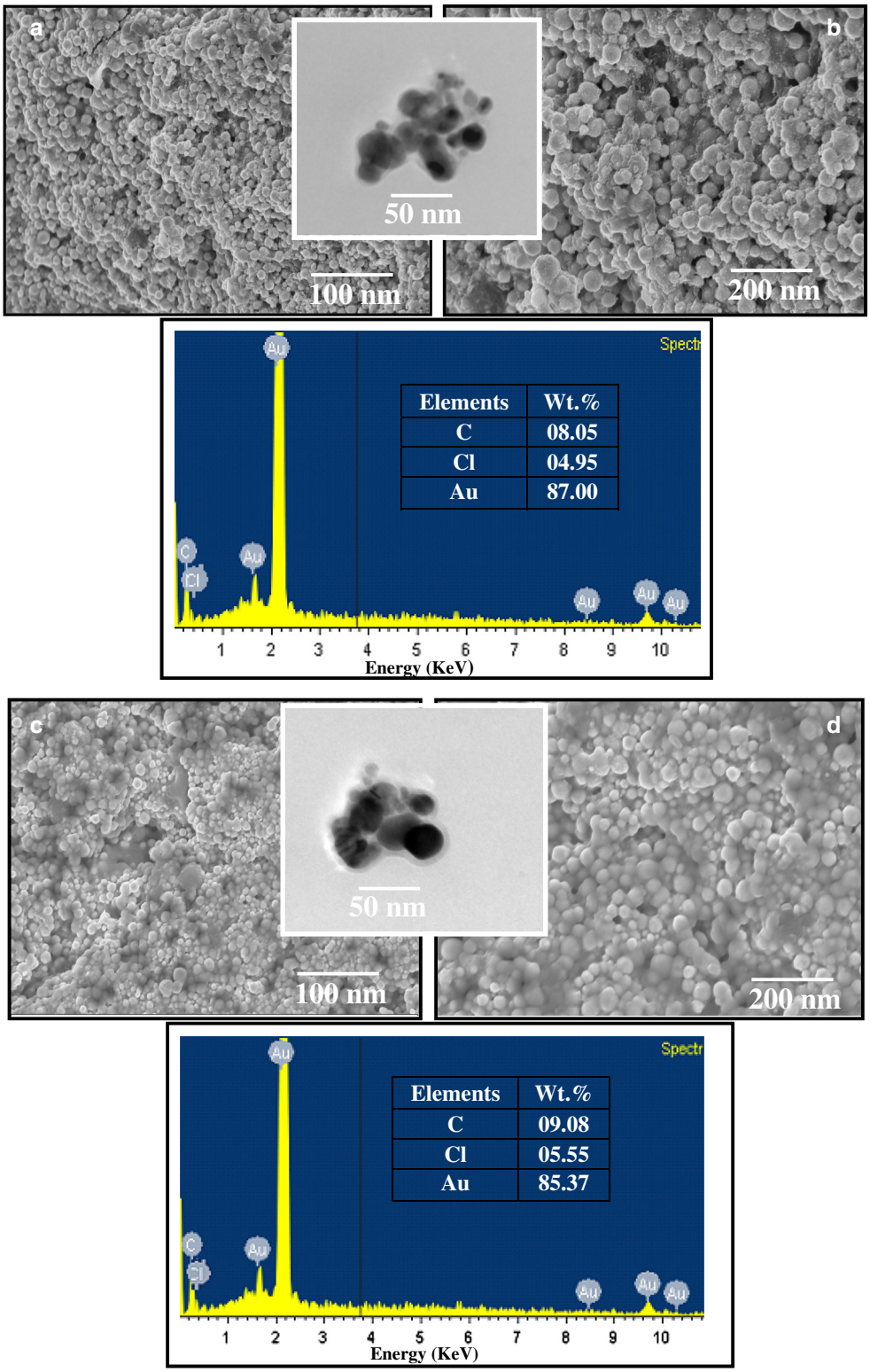

Fig. 6 FESEM (*inset* TEM) images and the corresponding EDX spectra of as synthesized AuNPs (**a**) and AuNPs–FA–NHS–DOX (**b**)

1436 cm^{-1} (=CO stretching of anhydride) bands in FT-IR spectra. A broad peak at 2915 cm^{-1} is a sign for bending of $–NH_2$ (secondary amines) and a peak at 3000 cm^{-1} signifies primary $–NH_2$. Overall, FT-IR spectra confirmed the conjugation of AuNPs with activated folic acid and drug molecules.

The cytotoxic effect of phytosynthesized AuNPs conjugated with FA and DOX were tested against different cell

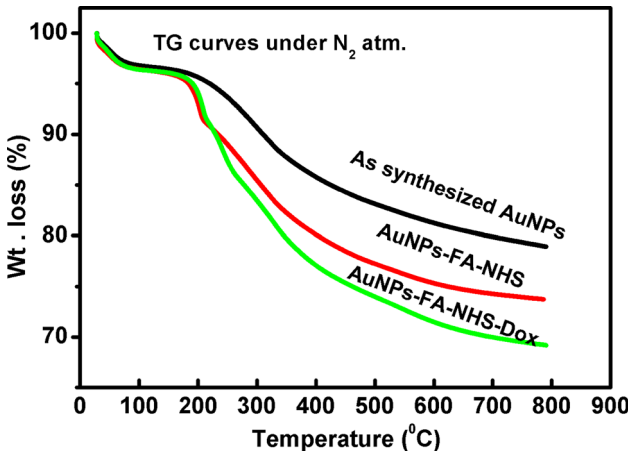

Fig. 7 TG curves of as synthesized AuNPs, AuNPs–FA–NHS and AuNPs–FA–NHS–DOX

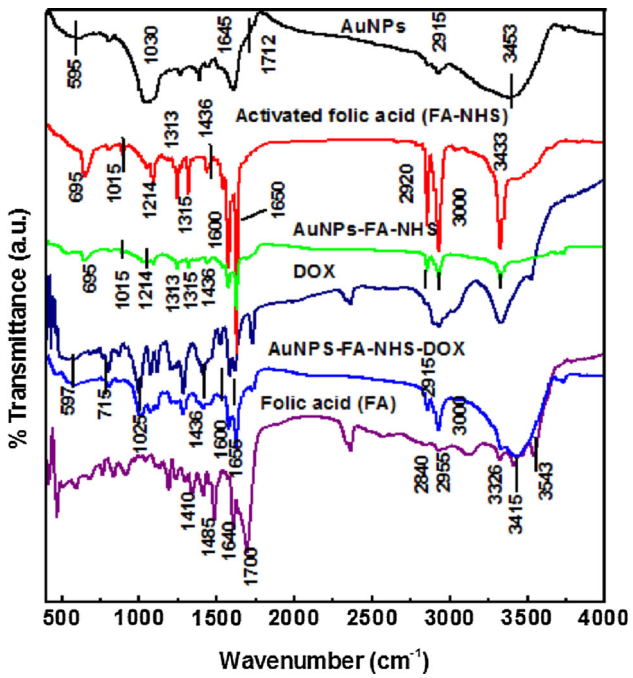

Fig. 8 FT-IR spectra of as synthesized AuNPs, folic acid, DOX, activated folic acid (FA–NHS), AuNPs–FA–NHS and AuNPs–FA–NHS–DOX

lines viz., MDA-MB-231, HeLa, SiHa and Hep-G2 (cancer cells) and Vero (normal cells). Figure 9 shows the impact of AuNPs, standard DOX drug and AuNPs–FA–NHS–DOX on normal and cancer cells after incubating for 24–72 h with different dose levels, 10–50 μg/ml. The viability of cells was found to decrease with increasing dose, 10–50 μg/ml as well as incubation time, 24–72 h. The cell viability of AuNPs at lower dose (10 μg/ml) was found to be ~83 % for both normal and cancer cells. However, there was a gradual decrease in the viability of cells with increasing dose of AuNPs. At a higher dose of 50 μg/ml, the viability of Vero, MDA-MB-231, HeLa, SiHa and Hep-G2 cells dropped to 59.4, 48.2, 47.1, 49.2 and 48.5 %, respectively, after 48 h exposure. The IC_{50} values and % inhibition of cell proliferation of AuNPs is shown in Table 1. This high cytotoxicity of AuNPs on human cancer cells is due to bio-capped organic moieties (phytochemicals) on the morphology, uniform size and shape [41]. On the other hand, normal epithelial Vero cells showed excellent biocompatibility for AuNPs here. This could be due to the presence of cell growth boosting factors in the *M. foeteda* leaves extract and the high content of phytochemicals (polyphenols, terpenoids, reducing sugars and other hydrophobic organic moieties) enable easy internalization of AuNPs via hydrophobic interior of the cell membrane [42]. A similar biocompatibility of AuNPs is observed in many studies [5, 43], however, the cytoxicity of AuNPs for cancer cells is influenced by their morphological features as well as type of cell lines [44, 45].

For comparison, the cytotoxic effect of std. DOX and AuNPs–FA–NHS–DOX on these normal and cancer cells was found to be considerably high at all the concentrations (10–50 μg/ml) here. For instance, at higher dose of 50 μg/ml DOX, the cell survival is found to be ~40 % for normal cells and ~35 % for cancer cells, which can be said to be extremely toxic for these tested cells. The IC_{50} values of DOX was found to be 30 μg/ml for Vero, MDA-MB-231, HeLa, SiHa and Hep-G2 cell lines, upon 48 h exposures. These results indicate the potential toxicity of DOX in chemotherapy. The cytotoxic effect of AuNPs–FA–NHS–DOX is much higher when compared to DOX and AuNPs alone. The cell viability was found to be ~50 % for normal cells and ~7 % for cancer cells at 50 μg/ml concentration of AuNPs–FA–NHS–DOX. For AuNPs and DOX, the cell viability was 59.4 and 40 % for normal cells and 48 and 35 % for cancer cell lines, respectively. The IC_{50} value of AuNPs–FA–NHS–DOX on normal and cancer cells was found to be 50 and 20 μg/ml respectively. Thus, AuNPs–FA–NHS–DOX is highly potent even at low dose level. Raghunandan et al. [46] have reported AuNPs as potential therapeutic carrier and highly useful in detection and destruction of cancer cells. Goodman et al. [47] have also reported the toxicity of AuNPs conjugated with different ligands on different cancer cells. Nevertheless, the detailed cell interaction studies on these nanomaterials are needed for understanding the exact mechanism. In comparison to standard DOX, the cytotoxicity of AuNPs–FA–NHS–DOX was found to be less on normal Vero cells and high on cancer cells. Thus, AuNPs–FA–NHS–DOX complex is relatively biocompatibility for normal cells probably due to the impact of potential targeting for cancer cells.

The main role of AuNPs–FA–NHS–DOX is on the sustained delivery of drug in an ideal tumor environment. Therefore, we have subjected AuNPs–FA–NHS–DOX for

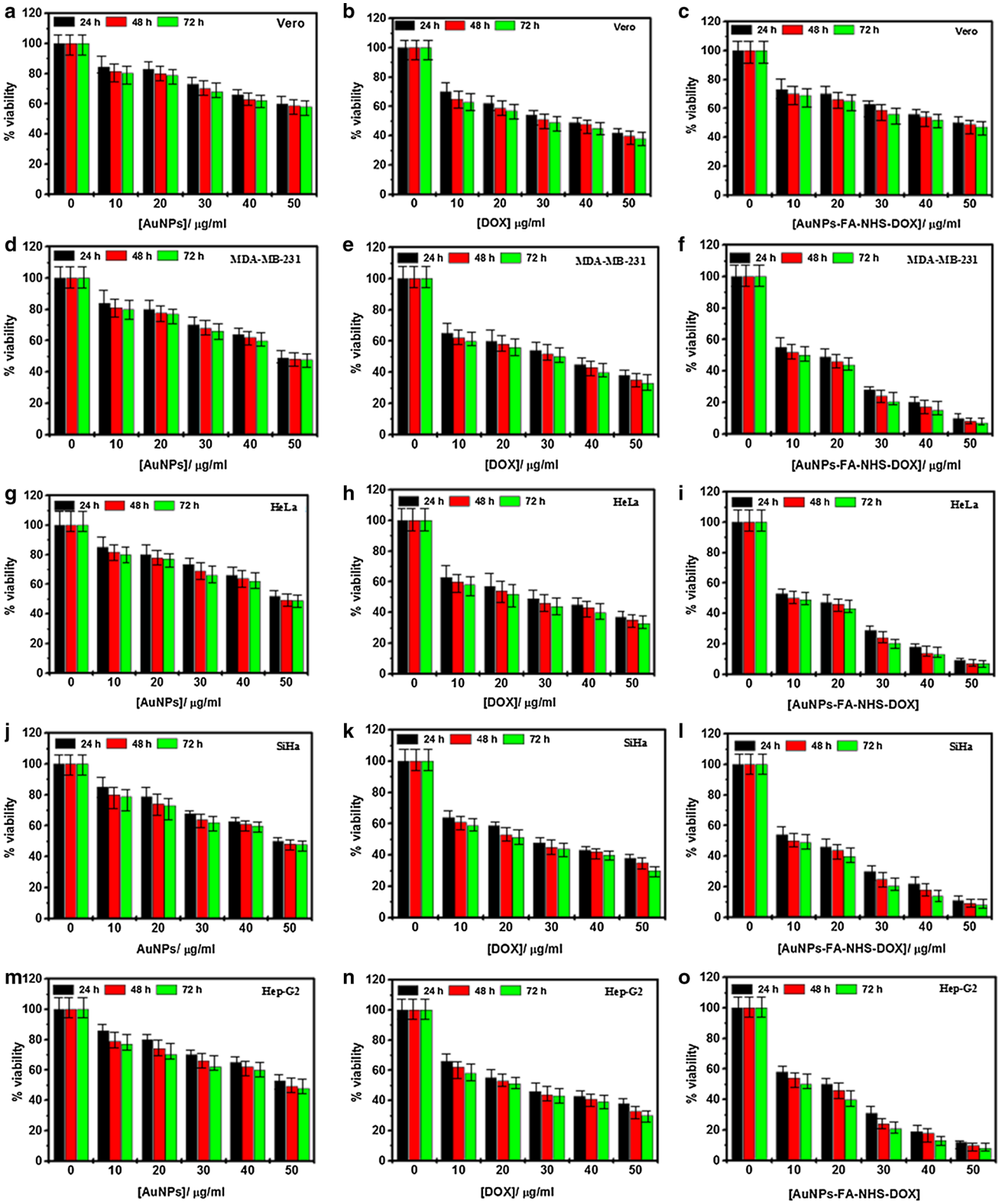

Fig. 9 Cell viability assays of Vero (**a**–**c**) MDA-MB-231 (**d**–**f**), HeLa (**g**–**i**), SiHa (**j**–**l**) and Hep-G2 (**m**–**o**) after exposure to different concentrations of AuNPs, DOX drug and AuNPs–FA–NHS–DOX at 24, 48 and 72 h. The values represent the mean ± standard deviation of three independent experiments (Color figure online)

Table 1 Growth-inhibitory effect (after 48 h) of AuNPs, DOX and AuNPs–FA–NHS–DOX

Treated samples	Inhibitory effect on cell lines (IC_{50})				
	Vero	MDA–MB–231	HeLa	SiHa	Hep–G2
AuNPs	60 μg/ml (50.05 %)	50 μg/ml (51.80 %)	50 μg/ml (52.90 %)	50 μg/ml (51.80 %)	50 μg/ml (51.50 %)
DOX	30 μg/ml (59.88 %)	30 μg/ml (53.56 %)	30 μg/ml (54.55 %)	30 μg/ml (52.40 %)	30 μg/ml (51.56 %)
AuNPs–FA–NHS–DOX	50 μg/ml (49.95 %)	20 μg/ml (54.40 %)	20 μg/ml (52.50 %)	20 μg/ml (53.60 %)	20 μg/ml (51.40 %)

Each value represents mean ± SD. The data was analyzed by Student's t test

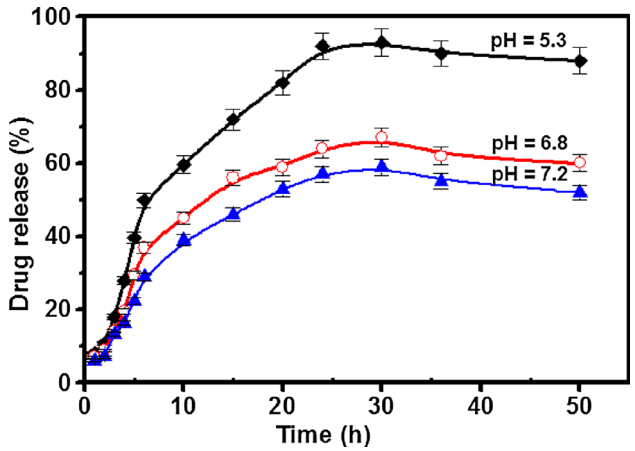

Fig. 10 Drug release profile of AuNPs–FA–NHS–DOX with time at different pH

drug release experiment using dialysis tube (cut-off = 1 kDa) in phosphate buffer solution at different pH (5.3, 6.8 and 7.2). The ratio of AuNPs to drug was kept at 10:1 (drug concentration = 1.0 mg/ml). As shown in Fig. 10, the efficient drug release profile was found at pH 5.3. This may be due to the hydrolysis of the non-covalent chemical interaction between AuNPs and DOX at slightly acidic pH [19]. The amount of drug release was highest at pH 5.3 followed by pH 7.2 and pH 6.8. This pH dependent tendency of drug release can act as dual pronged strategy for cancer chemotherapy. This is because, soon after injecting the AuNPs–FA–NHS–DOX, it will interacts with blood components at physiological pH 7.2 wherein DOX remains anchored to AuNPs. Upon entry into the cancer cells via an endocytic pathway, most of the drug is released in this tumor environment, wherein acidic pH (4.5–6.5 depending on the type of tumor) prevails.

4 Conclusions

A uniform spherical shaped AuNPs have been successfully prepared by using *M. foetida* leave extract as a bio-reductant. These AuNPs were found to be coated with phytochemicals from plant extract, and such a bio-capping was useful (acting as natural bio-linker) for subsequent conjugation with folic acid and DOX. The NHS activated folic acid and DOX were effectively conjugated to AuNPs forming AuNPs–FA–NHS–DOX. Such a drug carrier, AuNPs–FA–NHS–DOX is tested here against normal epithelial cells (Vero) and human cancer cells (MDA-MB-231, HeLa, SiHa and Hep-G2) in comparison with AuNPs and std. DOX. The drug conjugated AuNPs complex showed low toxicity towards normal epithelial cells and high toxicity towards human cancer cells. Furthermore, the amount of drug released was maximum at pH 5.3 (an ambient condition for intravenous cancer drugs) followed by pH 7.2 and pH 6.8. In summary, we have developed an efficient and biocompatible anti-proliferating agent, although further studies (in vivo) are required to understand the drug delivery mechanism.

Acknowledgments Authors thank Dr. S.P. Hegde of Green Gold Global Research Institute, Kumta, Karnataka (India) for experimental facility during this study. Mr. S. Yallappa gratefully acknowledges the financial support from Kuvempu University.

References

1. Irvani S. Green synthesis of metal nanoparticles using plants. Green Chem. 2011;13:2638–50.
2. Shabnum N, Saradhi PP. Photosynthetic electron transport system promotes synthesis of Au-nanoparticles. PLoS One. 2013;8(8): e7123.
3. Yamal G, Sarrmila P, Rao KS, Saradhi PP. Yeast Extract Mannitol medium and its constituents promote synthesis of Au nanoparticles. Process Biochem. 2013;48:532–8.
4. Dreaden EC, Alkilany AM, Huang X, Murphy CJ, El-Sayed MA. The golden age: gold nanoparticles for biomedicine. Chem Soc Rev. 2012;41:2740–79.
5. Kim C, Agasti SS, Zhu Z, Isaacs L, Rotello VM. Recognition-mediated activation of therapeutic gold nanoparticles inside living cells. Nat Chem. 2010;2(11):962–6.
6. Sperling RA, Gil PR, Zhang F, Zanella M, Parak WJ. Biological applications of gold nanoparticles. Chem Soc Rev. 2008;37: 1896–906.
7. Giljohann DA, Seferos DS, Daniel WL, Massich MD, Patel PC, Mirkin CA. Gold nanoparticles for biology and medicine. Angew Chem. 2010;49(19):3280–94.
8. Murphy CJ, Gole AM, Stone JW, Sisco PN, Alkilany AM, Goldsmith EC, Baxter SC. Gold nanoparticles in biology: beyond

toxicity to cellular imaging. Acc Chem Res. 2008;41(12): 1721–30.
9. Lee H, Lee K, Kim IK, Park TG. Synthesis, characterization, and in vivo diagnostic applications of hyaluronic acid immobilized gold nanoprobes. Biomaterials. 2008;29(35):4709–18.
10. Fadeel B, Bennett AE. Better safe than sorry: understanding the toxicological properties of inorganic nanoparticles manufactured for biomedical applications. Adv Drug Deliv Rev. 2010;62(3):362–74.
11. Sezgin E, Karatas OF, Cam D. Interaction of gold nanoparticles with living cells. Sigma. 2008;26:227–46.
12. Daniel MC, Astrue D. Gold nanoparticles: assembly, supramolecular chemistry, quantum-size-related properties, and applications toward biology, catalysis, and nanotechnology. Chem Rev. 2004; 104:293–346.
13. Masala O, Seshadri R. Synthesis routes for large volumes of nanoparticles. Annu Rev Mater Res. 2004;34:41–81.
14. Sau TK, Rogach AL. Nonspherical noble metal nanoparticles: colloid-chemical synthesis and morphology control. Adv Mater. 2010;22(16):1781–804.
15. Zhang X, Yan S, Tyagi RD, Surmapalli RY. Synthesis of nanoparticles by microorganisms and their application in enhancing microbiological reaction rates. Chemosphere. 2011;82(4):489–94.
16. Das RK, Brar SK. Plant mediated green synthesis: modified approaches. Nanoscale. 2013;5(21):10155–62.
17. Bhat R, Sharanabasava VG, Deshpande R, Shetti U, Sanjeev G, Venkataraman A. Photo-bio-synthesis of irregular shaped functionalized gold nanoparticles using edible mushroom *Pleurotus florida* and its anticancer evaluation. J Photochem Photobiol B. 2013;125:63–9.
18. Jiang X, Sun D, Zhang G, He N, Liu H, Huang J, Wubah TO, Li Q. Investigation of active biomolecules involved in the nucleation and growth of gold nanoparticles by *Artocarpus heterophyllus* Lam leaf extract. J Nanopart Res. 2013;15:1741–51.
19. Pandey S, Oza G, Mewada A, Shah R, Thakur M, Sharon M. Folic acid mediated synaphic delivery of doxorubicin using biogenic gold nanoparticles anchored to biological linkers. J Mater Chem B. 2013;1:1361–70.
20. Brigger I, Dubernet C, Couvreur P. Nanoparticles in cancer therapy and diagnosis. Adv Drug Deliv Rev. 2002;54:631–51.
21. Heegaard PM, Boas U, Otzen DE. Dendrimer effects on peptide and protein fibrillation. Macromol Biosci. 2007;7:1047–59.
22. Kamen BA, Capdevila A. Receptor-mediated folate accumulation is regulated by the cellular folate content. Proc Natl Acad Sci. 1986;83:5983–7.
23. Pan J, Feng SS. Targeted delivery of paclitaxel using folate-decorated poly(lactide)-vitamin E TPGS nanoparticles. Biomaterials. 2008;29:2663–72.
24. Wang S, Lee RJ, Mathias CJ, Green MA, Low PS. Synthesis, purification, and tumor cell uptake of 67 Ga-deferoxamine-folate, a potential radiopharmaceutical for tumor imaging. Bioconjugate Chem. 1996;7(1):56–62.
25. Steinberg G, Borch RF. Synthesis and evaluation of pteroic acid-conjugated nitroheterocyclic phosphoramidates as folate receptor-targeted alkylating agents. J Med Chem. 2001;44(1):69–73.
26. Rui Y, Wang S, Low PS, Thompson DH. Diplasmenylcholine-folate liposomes: an efficient vehicle for intracellular drug delivery. J Am Chem Soc. 1998;120:11213–8.
27. Douglas JT, Rogers BE, Rosenfeld ME, Michael SI, Feng M, Curiel DT. Targeted gene delivery by tropism-modified adenoviral vectors. Nat Biotechnol. 1996;14:1574–8.
28. Sharma S, Kumar A, Namdeo AG. Pharmacognostical and phytochemical analysis of nothapodytes nimmoniana stem. Int J Pharm Pharm Sci. 2012;4:455–9.
29. Lorence A, Craig LN. Camptothecin, over four decades of surprising findings. Phytochemistry. 2004;65:2731–841.
30. Prasenjit M, Mahua S, Parames CS. Aqueous extract of *Terminalia arjuna* prevents carbon tetrachloride induced hepatic and renal disorders. BMC Complement Altern Med. 2006;6:33–42.
31. Mulvaney P. Surface plasmon spectroscopy of nanosized metal nanoparticles. Langmuir. 1996;12:788–800.
32. Yallappa S, Manjanna J, Dhananjaya BL. Phytosynthesis of stable Au, Ag and Au-Ag alloy nanoparticles using *J. sambac* leaves extract, and their enhanced antimicrobial activity in presence of organic antimicrobials. Spectrochim Acta A. 2015;137:236–43.
33. Dauthal P, Mukhopadyay M. *Pruns domestica* fruit extract-mediated synthesis of gold nanoparticles and its catalytic activity for 4-nitrophenol reduction. Ind Eng Chem Res. 2012;51:13014–20.
34. Yallappa S, Manjanna J, Sindhe MA, Satyanarayan ND, Pramod SN, Nagaraja K. Microwave assisted rapid synthesis and biological evaluation of stable copper nanoparticles using *T. arjuna* bark extract. Spectrochim Acta A. 2013;110:108–15.
35. Long NN, Vu LV, Kiem CD, Doanh SC, Nguyer CT, Hang PT, Thien ND, Quynh LM. Synthesis and optical properties of colloidal gold nanoparticles. J Phys Conf Ser. 2007;187:012026.
36. Alexander CM, Hamner KL, Maye MM, Dabrowiak JC. Multifunctional DNA-gold nanoparticles for targeted doxorubicin delivery. Bioconjugate Chem. 2014;25:1261–71.
37. Hussain N, Jaitley V, Florence AT. Recent advances in the understanding of uptake of microparticulates across the gastrointestinal lymphatics. Adv Drug Deliv Rev. 2001;50:107–42.
38. Ankamwar B, Damle C, Ahmad A, Sastry M. Biosynthesis of gold and silver nanoparticles using Emblica Officinalis fruit extract, their phase transfer and transmetallation in an organic solution. J Nanosci Nanotechnol. 2005;5:1665–71.
39. Kholoud MM, El-Noura A, Eftaihab A, Al-Warthanb A, Ammar RAA. Synthesis and applications of silver nanoparticles. Arabian J Chem. 2010;3:135–40.
40. Shankar SS, Ahamad A, Pasricha R, Sastry M. Bioreduction of chloroaurate ions by geranium leaves and its endophytic fungus yields gold nanoparticles of different shapes. J Mater Chem. 2003;13:1822–6.
41. Kevin B. Shape of matters for nanoparticle technology. Cambridge: MIT Review; 2008.
42. Mewada A, Pandey S, Oza G, Shah R, Thakur M, Gupta A, Sharon M. A novel report on assessing pH dependent role of nitrate reductase on green biofabrication of gold nanoplates and nanocubes. J Bionanosci. 2013;7:174–80.
43. Connor EE, Mwamuka J, Gole A, Murphy CJ, Wyatt MD. Gold nanoparticles are taken up by human cells but do not cause acute cytotoxicity. Small. 2005;1:325–7.
44. Patra HK, Banerjee S, Chaudhuri U, Lahiri P, Dasgupta AK. Cell selective response to gold nanoparticles. Nanomed Nanotechnol Biol Med. 2007;3:111–9.
45. Pan Y, Neuss S, Leifert A, Fischler M, Wen F, Simon U, Schmid G, Brandau W, Jahnen-Dechent W. Size dependent cytotoxicity of gold nanoparticles. Small. 2007;3:1941–9.
46. Raghunandan D, Ravishankar B, Sharanabasava G, Mahesh DR, Harsoor V, Yatagatti MS, Bhagawanraju M, Venkataraman A. Anticancer studies of noble metal nanoparticles synthesized using different plant extracts. Cancer Nanotechnol. 2011;2:57–65.
47. Goodman CM, McCusker CD, Yilmaz T, Rotello VM. Toxicity of gold nanoparticles functionalized with cationic and anionic side chains. Bioconjugate Chem. 2004;15:897–900.